

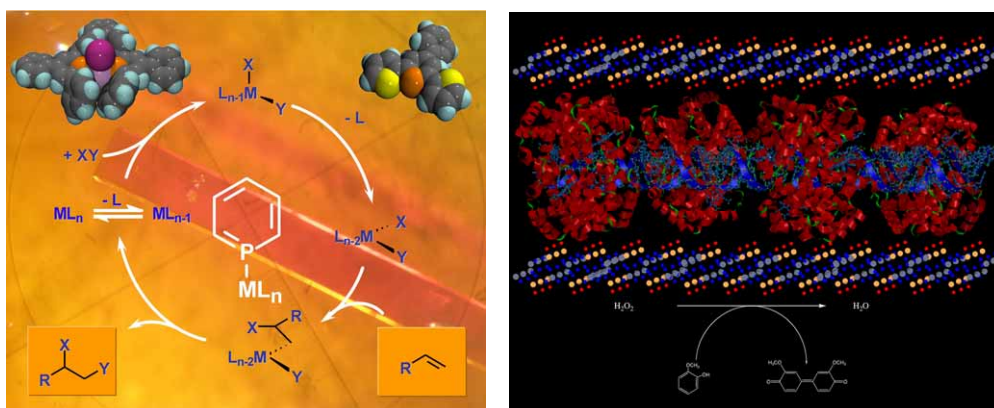
This paper is published as part of a *Dalton Transactions* themed issue on:

Emerging Strategies in Catalysis

Guest Edited by Carmen Claver
Universitat Rovira i Virgili, Tarragona



Published in [issue 47, 2007](#) of *Dalton Transactions*



Images reproduced by permission of Christian Muller (outside) and Challa Kumar (inside)

Other papers published in this issue include:

[Access to well-defined isolated Fe\(II\) centers on silica and their use in oxidation](#)

Charbel Roukoss, Steven Fiddy, Aimery de Mallmann, Nuria Rendón, Jean-Marie Basset, Emile Kuntz and Christophe Copéret, *Dalton Trans.*, 2007, DOI: [10.1039/b711015d](#)

[Phosphinines as ligands in homogeneous catalysis: recent developments, concepts and perspectives](#)

Christian Müller and Dieter Vogt, *Dalton Trans.*, 2007, DOI: [10.1039/b712456m](#)

[“Solventless” continuous flow homogeneous hydroformylation of 1-octene](#)

Anja C. Frisch, Paul B. Webb, Guoying Zhao, Mark J. Muldoon, Peter J. Pogorzelec and David J. Cole-Hamilton, *Dalton Trans.*, 2007, DOI: [10.1039/b712683b](#)

[Palladium catalyzed Suzuki C–C couplings in an ionic liquid: nanoparticles responsible for the catalytic activity](#)

Fernando Fernández, Beatriz Cordero, Jérôme Durand, Guillermo Muller, François Malbosc, Yolande Kihn, Emmanuelle Teuma and Montserrat Gómez, *Dalton Trans.*, 2007, DOI: [10.1039/b713449e](#)

Visit the *Dalton Transactions* website for cutting-edge inorganic research

www.rsc.org/dalton

Supported ionic liquid phase rhodium nanoparticle hydrogenation catalysts

Marcos A. Gelesky,^a Sandra S. X. Chiaro,^b Flávio A. Pavan,^a João H. Z. dos Santos^{*a} and Jairton Dupont^{*a}

Received 29th May 2007, Accepted 25th July 2007

First published as an Advance Article on the web 9th August 2007

DOI: 10.1039/b708111a

Rh(0) nanoparticles (*ca.* 4 nm) dispersed in an ionic liquid (1-*n*-butyl-3-methylimidazolium tetrafluoroborate) were immobilized within a silica network, prepared by the sol–gel method. The effect of the sol–gel catalyst (acid or base) on the encapsulated ionic liquid and Rh(0) content, on the silica morphology and texture, and on the catalyst alkene hydrogenation activity was investigated. The Rh(0) content in the resulting xerogels (*ca.* 0.1 wt% Rh/SiO₂) was shown to be independent of the sol–gel process. However, acidic conditions afforded higher contents of encapsulated ionic liquid and xerogels with larger pore diameters, which in turn might be responsible for the higher catalyst activity in hydrogenation of the alkenes.

Introduction

The combination of an ionic liquid with a solid support material is emerging as a new alternative for the immobilization of transition-metal catalyst precursors.^{1,2} This process named *Supported Ionic Liquid Phase* (SILP) catalysis is a concept which combines the advantages of ionic liquids with those of heterogeneous support materials. These materials are prepared by the covalent attachment of ionic liquids to the support surface or by simply depositing the catalytically active species-containing ionic liquid phases on the surface of a support, usually silica- or polymeric-based materials. In several cases, the procedure involves the simple dissolution of a sulfonated phosphine-modified rhodium catalyst into a supported ionic liquid, while the substrates constitute the organic phase. This method reduces the amount of ionic liquid and affords easy and efficient separation of products from the catalyst. In comparison to the traditional biphasic systems, higher catalytic activity and lower metal leaching can be obtained by the suitable tuning of the experimental conditions.^{1,3–7} The SILP systems have been used in various catalytic reactions such as Friedel–Crafts reactions,⁸ Rh-catalyzed hydroformylations⁶ and hydrogenations,⁹ Pd-catalyzed Heck reactions,¹⁰ and Rh-, Pd-, and Zn-catalyzed hydroaminations.¹¹

Imidazolium ionic liquids (ILs) possess pre-organized structures mainly through hydrogen bonds which induce structural directionality.¹² These IL structures can adapt or be adaptable to many species, as they provide hydrophobic or hydrophilic regions, and a high directional polarizability.^{13,14} This structural organization of ILs can be used as “entropic drivers” for spontaneous, well-defined and extended ordering of nanoscale structures. Indeed, the unique combination of adaptability towards other molecules and phases associated to the strong hydrogen-bond-driven structure makes ionic liquids potential key tools in the preparation of a new generation of chemical nanostructures^{15,16} such as templated porous silica prepared in a sol–gel process.^{17–19}

Moreover, *metal nanoparticles* (MNPs) with small diameter and narrow size distribution can be prepared by simple H₂ reduction of metal compounds or decomposition of organometallic species dissolved in ILs.^{20–22} Although these MNPs dispersed in ILs are catalysts for reactions under multiphase conditions, in several cases the MNPs are not stable and tend to aggregate.²³ Alternatively, these nanoparticles can be used in conjunction with other stabilizers or be easily transferred to other organic and inorganic supports to generate more stable and active catalysts.^{24–27} The nanoparticle/ionic liquid/stabilizer combination usually exhibits an excellent synergistic effect that enhances activity and robustness of the catalyst. Therefore, it is quite plausible to assume that more efficient and stable catalytic systems could be prepared by the generation of metal nanoparticles associated with silica using ILs as templates for both catalytic partners *i.e.* the metal nanoparticles and the silica support.^{28,29}

We present herein our results which show that imidazolium ionic liquids can be used for the generation of silica supported Rh(0) nanoparticles *via* sol–gel processes.

Experimental

General

Except for the preparation of the Rh(0) nanoparticles all experiments were performed in air. RhCl₃·3H₂O and Rh/C (5%) were provided by Degussa (Brazil). The halide free 1-*n*-butyl-3-methylimidazolium tetrafluoroborate (BMI.BF₄) ionic liquid³⁰ and the Rh(0) nanoparticles³¹ were prepared according to known procedures. Solvents and alkenes were dried with the appropriate drying agents and distilled under argon prior to use. All other chemicals were purchased from commercial sources and used without further purification. Gas chromatography analysis was performed with a Hewlett-Packard-5890 gas chromatograph with an FID detector and a 30 m capillary column with a dimethylpolysiloxane stationary phase.

The nanoparticle formation and hydrogenation reactions were carried out in a modified Fischer–Porter bottle immersed in a silicone oil bath and connected to a hydrogen tank. The temperature was maintained at 75 °C by a hot-stirring plate

^aLaboratory of Molecular Catalysis, Institute of Chemistry-UFRGS, P.O.Box 15003, 91501-970, Porto Alegre, RS, Brazil. E-mail: dupont@iq.ufrgs.br; Fax: +55 51 3308 7304; Tel: +55 51 3308 6321

^bPETROBRAS S.A. -R&D Center Quadra 7-Cidade Universitaria-Ilha do Fundão, 21949-900, Rio de Janeiro, RJ, Brazil

connected to a digital controller (ETS-D4 IKA) with stirring at 1200 rpm. The fall in the hydrogen pressure in the tank was monitored with a pressure transducer interfaced through a Novus converter to a PC and the data workup *via* Microcal Origin 5.0™.

Synthesis of Rh(0) nanoparticles immobilized in silica

Silica immobilized Rh(0) nanoparticles were prepared by the sol-gel method under acidic and basic conditions. Typical procedure for acid catalysis: 10 mL of tetraethoxy orthosilicate (9.34 g, 45 mmol) was introduced in a Becker under vigorous stirring at 60 °C. The Rh(0) nanoparticles (10 mg, 0.1 mmol) were dissolved in BMI.BF₄ (1 mL, 5.1 mmol) and ethanol (5 mL). This solution was submitted to stirring and sonication for 2 min and then added to the solution containing TEOS. Consecutively, an acid solution (HF or HCl) was added as acid catalyst. The temperature was kept at 60 °C for 18 h. The resulting material was washed several times with acetone and dried under vacuum.

Typical procedure for base catalysis: 10 mL of TEOS (9.34 g, 45 mmol) was added to ethanol (5 mL), containing the ionic liquid BMI.BF₄ (1 mL, 5.1 mmol) and previously isolated Rh(0) nanoparticles (10 mg, 0.1 mmol). Then ethanol (95 mL) and ammonium hydroxide (20 mL) were added. The mixture was kept under stirring for 3 h at room temperature and left to stand for a further 18 h. The resulting xerogel was filtered and washed with acetone and dried under vacuum for 1 h.

Elemental analysis (CHN)

The organic phases present in the xerogels were analyzed using CHN elemental Perkin Elmer elemental CHNS/O analyzer, model 400. Triplicate analysis of the samples, previously heated at 100 °C under vacuum for 1 h, was carried out.

Rutherford Backscattering Spectrometry (RBS)

Rhodium loadings in catalysts were determined by RBS using He⁺ beams of 2.0 MeV incident on homogeneous tablets of the compressed (12 MPa) catalyst powder. The method is based on the determination of the number and energy of the detected particles which are elastically scattered in the Coulombic field of the atomic nuclei in the target. In this study, the Rh/Si atomic ratio was determined by the heights of the signals corresponding to each of the elements in the spectra and converted to wt% Rh(0)/SiO₂. For an introduction to the method and applications of this technique the reader is referred elsewhere.³²

Nitrogen adsorption-desorption isotherms

The adsorption-desorption isotherms of previous degassed solids (150 °C) were determined at liquid nitrogen boiling point in a volumetric apparatus, using nitrogen as probe. The specific surface areas of xerogels were determined from the *t*-plot analysis and pore size distribution was obtained using the BJH method. A homemade equipment with a vacuum line system employing a turbo-molecular Edwards vacuum pump was used. The pressure measurements were made using a capillary Hg barometer and a Pirani gauge.

Scanning Electron Microscopy (SEM) and Electron Dispersive Spectroscopy (EDS) elemental analysis

The materials were analyzed by SEM using a JEOL model JSM 5800 with 20 kV and 5000 magnification. The same instrument with was used for the EDS with a Noran detector (20 kV and acquisition time of 100 s and 5000 magnification).

Transmission Electron Microscopy (TEM) analysis

The morphologies and the electron diffraction (ED) patterns of the obtained particles were determined on a JEOL JEM-2010 equipped with an EDS system and a JEOL JEM-120 EXII electron microscope, operating at accelerating voltages of 200 and 120 kV, respectively. The TEM samples were prepared by deposition of the Rh(0) nanoparticles or Rh(0)/SiO₂ isopropanol dispersions on a carbon-coated copper grid at room temperature. The histograms of the nanoparticle size distributions were obtained from the measurement of around 300 diameters and reproduced in different regions of the Cu grid assuming spherical shapes.

Hydrogenations

The catalysts (100 mg) were placed in a Fischer-Porter bottle and the alkene (12.5 mmol) was added. The reactor was placed in an oil bath at 75 °C and hydrogen was admitted to the system at constant pressure (4 atm) under stirring until the consumption of hydrogen stopped. The organic products were recovered by decantation and analyzed by GC. The re-use of the catalysts were performed by simple extraction of the organic phase (upper phase) followed by the addition of the alkene. After ten recycles the solid was isolated, re-dispersed in isopropanol and placed in a cooper carbon grid.

Results and discussion

The sol-gel process allows us to obtain solid products by creating an oxide network *via* progressive polycondensation reactions of molecular precursors in a liquid medium. This process is considered as a soft chemical (*chimie douce*) approach for the synthesis of metastable (amorphous) oxide materials.³³ The process essentially comprehends two steps: hydrolysis and condensation. Both reactions are affected by the nature of the catalyst. Therefore, in the present study, two main routes were evaluated: (i) an acid-catalyzed one using either HF or HCl, and (ii) a base-catalyzed approach, using NH₄OH as catalyst. In both routes, the hydrolysis and condensation of tetraethoxy orthosilicate (TEOS) were performed in the presence of Rh(0) nanoparticles, which were prepared by hydrogen reduction (4 atm) of RhCl₃·*n*H₂O dissolved in the hydrophilic 1-*n*-butyl-3-methylimidazolium tetrafluoroborate ionic liquid at 75 °C. The hydrophilic 1-*n*-butyl-3-methylimidazolium tetrafluoroborate ionic liquid was selected for this study in order to guarantee the complete solubilization of the aqueous base and acid catalysts. These nanoparticles of 4.8 nm were isolated and re-dispersed in the ionic liquid. Table 1 presents the elemental analysis of the resulting silicas.

Carbon and nitrogen content was taken as a sign for the presence of ionic liquid BMI.BF₄ once encapsulated within the silica network. According to Table 1, higher ionic liquid contents were incorporated with the acid catalysts. It is worth noting that in the case of acidic conditions, hydrolysis is faster than condensation.

Table 1 Elemental analysis of Rh(0)/SiO₂

Sample	C/mmol g ⁻¹	N/mmol g ⁻¹	Rh(0) (%) ^a
Rh(0)/SiO ₂ /HF	16.3	4.2	0.11
Rh(0)/SiO ₂ /HCl	13.9	3.5	—
Rh(0)/SiO ₂ /NH ₄ OH	6.7	1.7	0.14

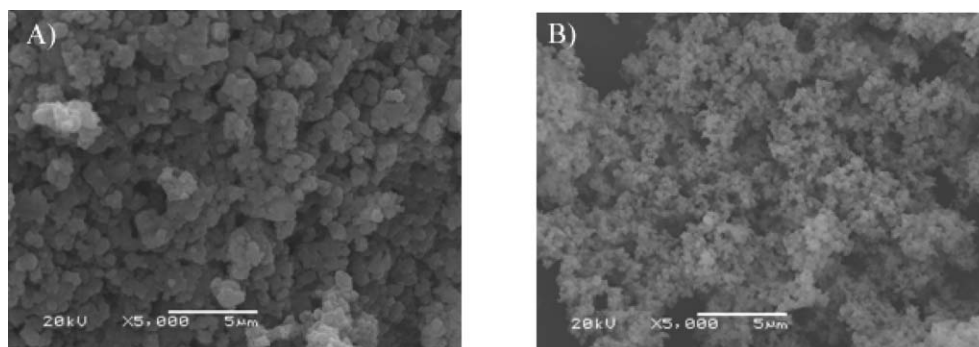
^a Determined by RBS.

The rate of condensation slows down with increasing number of siloxane linkages around a central silicon atom. This leads to weakly branched polymeric networks. On the other hand, in the case of basic conditions, condensation is accelerated relative to hydrolysis. The rate of condensation increases with increasing number of siloxane bridges. Thus, highly branched networks result.³⁴ In the present case, based on the carbon and nitrogen contents, it seems that the resulting weakly branched structure generated in the presence of acid catalyst (either HF or HCl) guarantees the constraint of the ionic liquid.

Metal contents were determined by Rutherford backscattering spectrometry (RBS). According to Table 1, the immobilized Rh content is roughly the same for silica prepared by both routes, corresponding to *ca.* 60–75% of the initial Rh content employed in the synthesis.

The metal distribution was determined by SEM-EDX analyses. Mapping showed a homogeneous Rh distribution in the silica grains, independently of the preparative route.

Fig. 1 illustrates the micrography of Rh(0)/SiO₂ prepared by both routes. According to Fig. 1, particle morphologies are in accordance to that usually observed for pure silica synthesized by these routes. In the case of acid-catalyzed conditions, a less organized, plate-like structure was observed, while in the case of basic conditions, spherical particles were obtained. It is worth noting that smaller particles were produced in the latter case. TEM was also employed for the characterization of the supported catalyst. Fig. 2a shows the micrograph of the isolated Rh(0) particles, the mean size of which was shown to be *ca.* 4.8 nm. In the case of Rh(0)/SiO₂ prepared by acid catalysis (HF), both the morphology and size (*ca.* 4.1 nm) were maintained within the silica framework. It is very likely that the presence of ionic liquid affords stability, avoiding sintering of the metallic particles. The same behavior was observed for the material prepared by the base catalysis.

**Fig. 1** Micrographs obtained by SEM of the resulting xerogels: (A) Rh(0)/SiO₂/HF and (B) Rh(0)/SiO₂/NH₄OH.

The textural properties were further characterized by nitrogen adsorption. Specific area was calculated by the BET method, while pore diameter, by the BJH one (Table 2). According to Table 2, silicas prepared in the absence of Rh(0) present higher specific area (*ca.* 100 m² g⁻¹). The introduction of metal particles during the synthesis led to a reduction in the specific area, independently of the synthetic route. The pore volume was shown to be independent of the presence or not of Rh(0) and of acidic or basic conditions. Nevertheless, the pore diameter was shown to be smaller for the materials prepared in the presence of NH₄OH as catalyst.

The supported catalysts were evaluated in hydrogenation reactions of aliphatic compounds. Table 3 presents data regarding 1-decene and cyclohexene hydrogenation reactions. For comparative purposes we also included the data concerning the catalytic activity of commercial Rh/C and of isolated Rh(0) nanoparticles.

Table 2 Textural properties of the xerogels^a

Entry	Sample	S _{BET} /m ² g ⁻¹	V _p /cm ³ g ⁻¹	d _p /nm
1	SiO ₂ /BMI.BF ₄ /HF	106	0.13	8.4
2	SiO ₂ /BMI.BF ₄ /NH ₄ OH	96	0.11	4.2
3	Rh(0)/SiO ₂ /HF	65	0.11	7.8
4	Rh(0)/SiO ₂ /NH ₄ OH	64	0.10	3.4

^a S_{BET} = specific area determined by BET method, V_p = pore volume, d_p = pore diameter.

Table 3 Hydrogenation of alkenes by encapsulated Rh(0) nanoparticles, Rh(0) nanoparticles and Rh/C^a

Entry	Catalyst	Alkene	t/min	TOF/min ^{-1b}
1	Rh(0)/SiO ₂ /HF ^c	1-Decene	22	54
2	Rh(0)/SiO ₂ /HF ^c	Cyclohexene	50	24
3	Rh(0)/SiO ₂ /NH ₄ OH ^d	1-Decene	60	16
4	Rh(0)/SiO ₂ /NH ₄ OH ^d	Cyclohexene	120	8
5	Rh(0) ^e	1-Decene	40	5
6	Rh(0) ^f	Cyclohexene	70	6
7	Rh/C ^g	1-Decene	21	31
8	Rh(0)/SiO ₂ /HF in BMI.BF ₄	1-Decene	740	0.8

^a Reaction conditions: temperature 75 °C; P_{H₂} (4 atm, constant pressure); conversion (100%); ^b Turnover frequency defined as mol hydrogenated product per mol of Rh(0) catalyst per minute; ^c (1) Rh(0)/SiO₂/HF (100 mg, 0.11% of Rh(0)) 12.5 mmol of alkene; ^d (2) Rh(0)/SiO₂/NH₄OH (100 mg, 0.14% of Rh(0)) 12.5 mmol of alkene; ^e Rh(0) nanoparticles (3 mg, 0.03 mmol), 6.25 mmol of alkene; ^f Rh(0) nanoparticles (3 mg, 0.03 mmol), 12.5 mmol of alkene; ^g 20 mg of Rh/C (5%), 6.25 mmol of alkene.

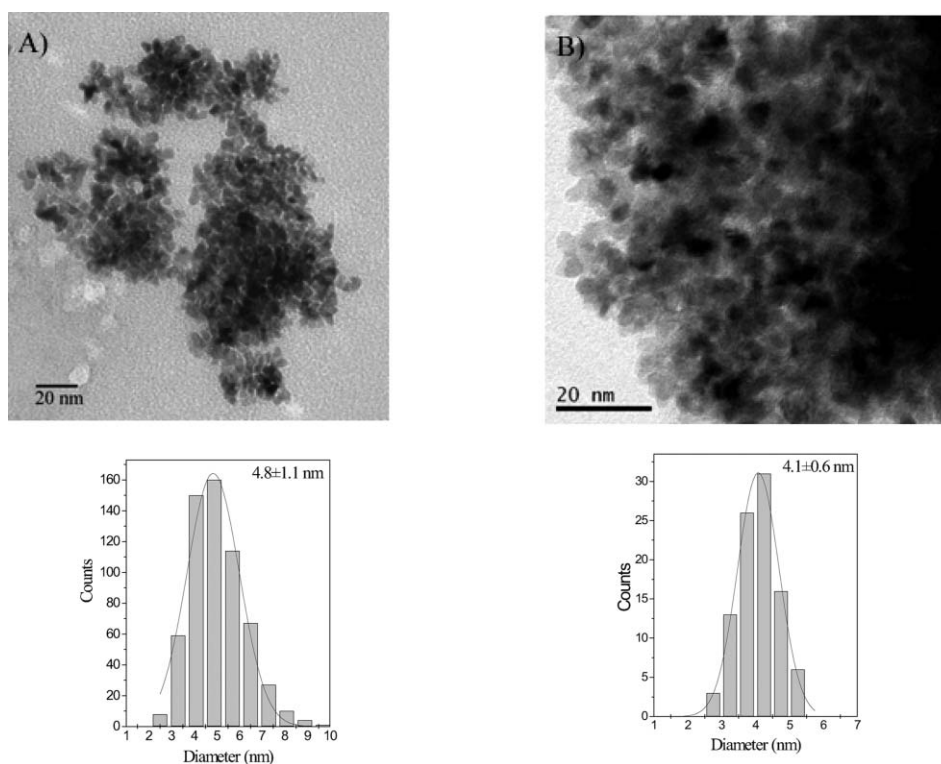


Fig. 2 Micrographs obtained by TEM of: (A) Rh(0) nanoparticles isolated from the ionic liquid and re-dispersed in isopropanol and (B) Rh(0)/SiO₂/HF.

As shown in Table 3, all the supported systems were more active than those constituted of isolated Rh(0) nanoparticles. Among the silica-based systems, those prepared under acidic conditions are the most active, exhibiting higher TOF in comparison to those of commercial Rh/C. The denser and bulkier structure generated under basic conditions might have afforded less active systems as shown by some clues. First, the ionic liquid content, which seems to be important in order to guarantee stability for the nanoparticles, was lower for these systems. Besides, according to porosimetric measurements, the pore diameter was much smaller for the Rh(0)/SiO₂/NH₄OH system. Rh(0) encapsulated particles, in spite of a slightly higher content in comparison to that afforded with an acid catalyst (see Table 1), might be not accessible in the supported systems prepared under basic conditions.

The hydrogenation of simple alkenes by Rh(0)/SiO₂/HF depends on steric hindrance at the C=C double bond and follows the same trend as observed with classical rhodium complexes in homogeneous conditions, that is, the reactivity follows the order: terminal-internal. This is exemplified in Fig. 3 which shows the conversion rate of 1-hexene and cyclohexene hydrogenation. Finally, the catalytic material can be recovered by simple decantation and re-used at least ten times without any significant loss in catalytic activity. The recovered material shows no sign of agglomeration as observed from the TEM analysis of Rh(0)/SiO₂/HF catalyst isolated after ten recharges (Fig. 4).

Conclusions

The Rh(0) nanoparticles dispersed in ionic liquid (1-*n*-butyl-3-methylimidazolium tetrafluoroborate) can be easily immobilized within a silica network when prepared by the sol-gel method (acid

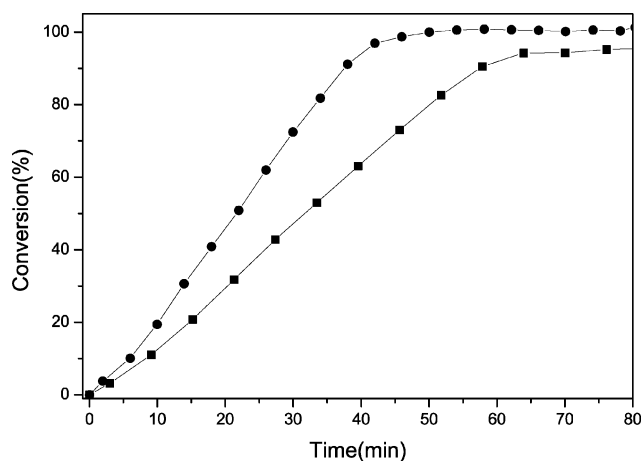


Fig. 3 Hydrogenation of 1-hexene (●) and cyclohexene (■) by Rh(0)/SiO₂/HF under 4 atm (constant pressure) at 75 °C, and [Alkene]/[Rh(0)] = 1179.

or base catalysis). The Rh(0) content in the resulting xerogels was shown to be independent of the preparative route, but acidic conditions afforded higher encapsulated ionic liquid content and xerogels with larger pore diameter, which in turn might have guaranteed higher catalyst activity in the hydrogenation of alkenes. The use of ionic liquid for the preparation of both nanoparticles and silica affords encapsulated ionic liquid/Rh(0)/silica materials with different morphology, texture, and catalytic activity. This combination exhibits an excellent synergistic effect that enhances the activity and robustness of the Rh hydrogenation catalysts.

All the supported systems were more active than that constituted of isolated Rh(0) nanoparticles for the hydrogenation of alkenes.

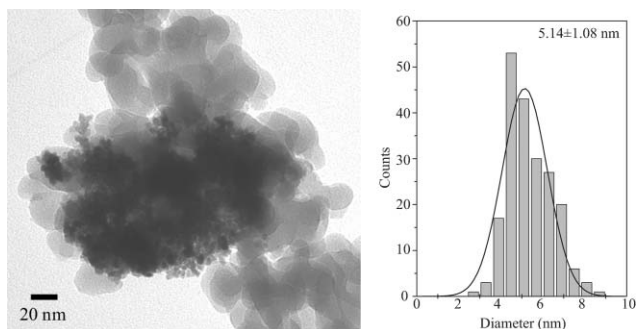


Fig. 4 Micrographs obtained by TEM of Rh(0)/SiO₂/HF isolated after ten re-cycles (1-decene hydrogenation).

In particular the silica-based systems prepared under acidic conditions were shown to be the most active, exhibiting higher TOF in comparison to that of commercial Rh/C (5%). The denser and bulkier silica structure generated under basic conditions (less active catalytic system) incorporated less ionic liquid. A high level of ionic liquid incorporation seems to be important in order to guarantee stability for the nanoparticles.

Acknowledgements

Thanks are due to the following agencies: CNPq, PETROBRAS and CT-PETRO for financial support and CME-UFRGS for the TEM and SEM microscopy analyses. We also thank Prof. H. S. Schrekker for proof reading of the manuscript.

Notes and references

- 1 C. P. Mehnert, *Chem.–Eur. J.*, 2004, **11**, 50–56.
- 2 A. Riisager, R. Fehrmann, M. Haumann and P. Wasserscheid, *Top. Catal.*, 2006, **40**, 91–102.
- 3 C. Bianchini and G. Giambastiani, *Chemtracts*, 2003, **16**, 301–309.
- 4 A. Riisager, R. Fehrmann, M. Haumann and P. Wasserscheid, *Eur. J. Inorg. Chem.*, 2006, 695–706.
- 5 C. L. Feng, Y. H. Wang and Z. L. Jin, *Prog. Chem.*, 2005, **17**, 209–216.
- 6 C. P. Mehnert, R. A. Cook, N. C. Dispenziere and M. Afeworki, *J. Am. Chem. Soc.*, 2002, **124**, 12932–12933.
- 7 P. B. Webb, T. E. Kunene and D. J. Cole-Hamilton, *Green Chem.*, 2005, **7**, 373–379.

- 8 C. deCastro, E. Sauvage, M. H. Valkenberg and W. F. Holderich, *J. Catal.*, 2000, **196**, 86–94.
- 9 C. P. Mehnert, E. J. Mozeleski and R. A. Cook, *Chem. Commun.*, 2002, 3010–3011.
- 10 H. Hagiwara, Y. Sugawara, K. Isobe, T. Hoshi and T. Suzuki, *Org. Lett.*, 2004, **6**, 2325–2328.
- 11 S. Breitenlechner, M. Fleck, T. E. Muller and A. Suppan, *J. Mol. Catal. A: Chem.*, 2004, **214**, 175–179.
- 12 J. Dupont and P. A. Z. Suarez, *Phys. Chem. Chem. Phys.*, 2006, **8**, 2441–2452.
- 13 C. S. Consorti, P. A. Z. Suarez, R. F. de Souza, R. A. Burrow, D. H. Farrar, A. J. Lough, W. Loh, L. H. M. da Silva and J. Dupont, *J. Phys. Chem. B*, 2005, **109**, 4341–4349.
- 14 J. Dupont, *J. Braz. Chem. Soc.*, 2004, **15**, 341–350.
- 15 M. Antonietti, D. B. Kuang, B. Smarsly and Z. Yong, *Angew. Chem., Int. Ed.*, 2004, **43**, 4988–4992.
- 16 Y. Zhou and M. Antonietti, *J. Am. Chem. Soc.*, 2003, **125**, 14960–14961.
- 17 Y. Zhou, J. H. Schattka and M. Antonietti, *Nano Lett.*, 2004, **4**, 477–481.
- 18 Y. Zhou, *Cur. Nanosc.*, 2005, **1**, 35–42.
- 19 S. Dai, Y. H. Ju, H. J. Gao, J. S. Lin, S. J. Pennycook and C. E. Barnes, *Chem. Commun.*, 2000, 243–244.
- 20 C. W. Scheeren, G. Machado, S. R. Teixeira, J. Morais, J. B. Domingos and J. Dupont, *J. Phys. Chem. B*, 2006, **110**, 13011–13020.
- 21 E. T. Silveira, A. P. Umpierre, L. M. Rossi, G. Machado, J. Morais, G. V. Soares, I. L. R. Baumvol, S. R. Teixeira, P. F. P. Fichtner and J. Dupont, *Chem.–Eur. J.*, 2004, **10**, 3734–3740.
- 22 J. Dupont, G. S. Fonseca, A. P. Umpierre, P. F. P. Fichtner and S. R. Teixeira, *J. Am. Chem. Soc.*, 2002, **124**, 4228–4229.
- 23 J. Dupont and P. Migowski, *Chem.–Eur. J.*, 2007, **13**, 32–39.
- 24 X. D. Mu, D. G. Evans and Y. A. Kou, *Catal. Lett.*, 2004, **97**, 151–154.
- 25 X. D. Mu, J. Q. Meng, Z. C. Li and Y. Kou, *J. Am. Chem. Soc.*, 2005, **127**, 9694–9695.
- 26 S. D. Miao, Z. M. Liu, B. X. Han, J. Huang, Z. Y. Sun, J. L. Zhang and T. Jiang, *Angew. Chem., Int. Ed.*, 2006, **45**, 266–269.
- 27 J. Huang, T. Jiang, B. X. Han, W. Z. Wu, Z. M. Liu, Z. L. Xie and J. L. Zhang, *Catal. Lett.*, 2005, **103**, 59–62.
- 28 V. Mevellec, A. Nowicki, A. Roucoux, C. Dujardin, P. Granger, E. Payen and K. Philippot, *New J. Chem.*, 2006, **30**, 1214–1219.
- 29 K. Zhu, F. Pozgan, L. D'Souza and R. M. Richards, *Microporous Mesoporous Mater.*, 2006, **91**, 40–46.
- 30 C. C. Cassol, G. Ebeling, B. Ferrera and J. Dupont, *Adv. Synth. Catal.*, 2006, **348**, 243–248.
- 31 G. S. Fonseca, A. P. Umpierre, P. F. P. Fichtner, S. R. Teixeira and J. Dupont, *Chem.–Eur. J.*, 2003, **9**, 3263–3269.
- 32 F. C. Stedile and J. H. Z. dos Santos, *Phys. Status Solidi A*, 1999, **173**, 123–134.
- 33 U. Schubert, N. Husing, *Inorganic Materials: A Chemical Approach*, 1st edn, Wiley, Weinheim, 2000.
- 34 *Characterization and Chemical Modification of the Silica Surface. (Studies in Surface Science and Catalysis, vol. 93)*, ed. E. F. Vansant, P. Van Der Voort and K. C. Vrancken, Elsevier, Amsterdam, 1995.